

Role of high-order Fourier terms for stability of monolayer-surface structures: Numerical simulations

Alexandre Tkatchenko*

Departamento de Química, División de Ciencias Básicas e Ingeniería, Universidad Autónoma Metropolitana-Iztapalapa, San Rafael Atlixco 186, Vicentina, AP. 55-534, México D.F. 09340, México

(Received 2 August 2006; revised manuscript received 5 September 2006; published 26 December 2006)

The role of high-order atom-surface Fourier terms is analyzed for the monolayer with coverage $\theta = \frac{3}{7}$ on (111) surface in cells with variable number of adsorbate atoms, allowed to relax to obtain the global minimum in each of the unit cells. A Fourier expansion with one or two shells of reciprocal cell vectors is used and three different models for the lateral interactions in the monolayer are tested, from purely repulsive to a real HFD-B2 potential. It is found that the simple commensurate $(\sqrt{7} \times \sqrt{7})R19.1^\circ$ three-atom structure is the most stable only when the contribution of the second Fourier term is included. In contrast to the conventional view, higher corrugation of the single-term Fourier model favors incommensurability. Evidence is collected that the high-order Fourier terms are mandatory for the stabilization of commensurate structures of an infinite monolayer.

DOI: 10.1103/PhysRevB.74.235440

PACS number(s): 68.35.-p, 68.43.Fg

I. INTRODUCTION

The stable structures of a monolayer-surface system can be classified into many different categories in respect to the monolayer orientation on the substrate surface or the minimum unit cell size.^{1,2} The complexity in stable structures is a result of subtle competition between the adsorbate-substrate forces and the lateral interactions between the atoms in the monolayer. The commensurate structures form one of those categories and they could be characterized by having a defined repeating unit cell unlike incommensurate structures, which could be defined by interatomic distance and rotation angle respective to the underlying substrate but possess no defined repeating pattern, as has been theoretically predicted by Novaco and McTague.^{3,4}

Many real monolayer-surface systems have been shown to form commensurate structures with different degree of symmetry. Probably the most illustrative examples are the rare-gas, halogen, and alkali monolayers on metal surfaces. For recent reviews of these cases see, e.g., Refs. 5–7. The ground state of monolayers on the (100) face of fcc crystals has been a subject of intense study,^{8,9} however, much less is known about the ground state structures of monolayers on the hexagonal (111) face. Moreover, the study of commensurate structures could be important for technological applications of wide amount of knowledge collected up to date for ordered monolayer-surface systems.¹⁰

A natural way of representing the interaction potential of an atom with a surface is the Fourier expansion with the reciprocal unit cell vectors¹¹

$$V(\mathbf{r}) = V_0(z) + \sum_{\mathbf{G}} V_{\mathbf{G}}(z) \exp(-i\mathbf{G} \cdot \mathbf{r}), \quad (1)$$

where \mathbf{r} is the real space vector, \mathbf{G} is the reciprocal space vector, and $V_{\mathbf{G}}(z)$ are the Fourier coefficients. Although the $V_{\mathbf{G}}(z)$ coefficients usually depend on the vertical position of the atom on top of the surface, in this paper the quasi-two-dimensional x - y representation of the Fourier series is used, where each $V_{\mathbf{G}}$ value is taken at the equilibrium z position. For physisorption systems the Fourier coefficients usually

decay very rapidly,¹² therefore it has often been assumed that the first coefficient— V_{G_0} —is sufficient for description of the monolayer-surface interaction in physisorption systems. Furthermore, it is known^{13,14} that when V_{G_0} is sufficiently large, a commensurate structure with one atom per unit cell is the ground state of the monolayer-surface system.¹⁵ At first glance it would also seem that an increase of V_{G_0} makes the higher-order commensurate structures, with several atoms locked into high-symmetry sites, stable. Namely, it has been proposed that a devil's staircase (an ordered sequence of high-order commensurate structures) could exist due to the increased corrugation of the monolayer-surface potential on the basis on experimental observations for the Ar-Pt(111) system.¹⁶ The variation of the atom-surface corrugation potential for different low-index surfaces [e.g., (100), (110), and (111)] can also affect the nature of the monolayer structures, as has been shown experimentally for Xe adlayers on Cu surfaces. Namely, the structures range from simple commensurate for Xe-Cu(111),¹⁷ to high-order commensurate (HOC) for Xe-Cu(110),¹⁸ to incommensurate for Xe-Cu(100).¹⁹

Recently, it has been shown analytically that for an infinite rigid hexagonal monolayer, each Fourier term in Eq. (1) contributes to stability of specific high-order commensurate structures, i.e., every Fourier term contributes to stability of commensurate structures with one atom per unit cell, while third and fifth terms contribute in the case of commensurate structures with three atoms per unit cell. For detailed analysis of this case, see Ref. 20. One conclusion of that study was that the first Fourier term (presumably the most important one) vanishes in the neighborhood of rigid hexagonal commensurate structures with more than one atom per unit cell. Therefore, one natural question is whether the HOC structures could be stabilized by the first Fourier term or they are exclusively seen due to the effect of the higher-order terms. Also, evidence exists that high-order Fourier terms contribute appreciably to the frequency gap of the commensurate monolayer.²¹

The role of higher Fourier terms for stability of monolayer-surface structures is analyzed in detail in the

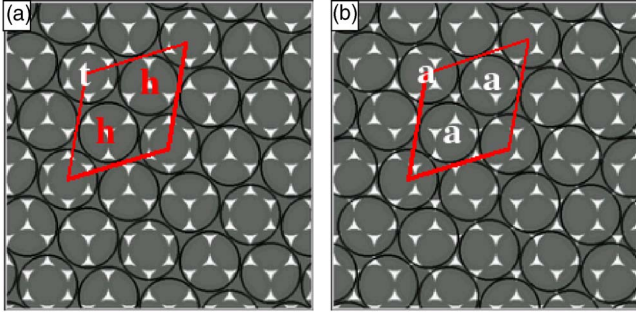


FIG. 1. (Color online) Models of two structures in the $(\sqrt{7} \times \sqrt{7})R19.1^\circ$ unit cell. The filled gray circles indicate the substrate atoms [(111) surface], while bigger black circles show adsorbed monolayer atoms. The unit cell is marked by a red (dark gray) rhomb in both cases. (a) Corrugated structure with one atom positioned on top site (marked by t) and two atoms in the hollow three-fold sites (marked by h). (b) Flat structure with three atoms on geometrically equivalent asymmetric sites (marked by a).

present work. It will be shown that for a model that includes only the first shell of reciprocal cell vectors (first Fourier component), there exists a higher-order commensurate structure with same coverage as the simple commensurate $(\sqrt{7} \times \sqrt{7})R19.1^\circ$ structure, and which has lower energy. Surprisingly, the larger the value of the first Fourier amplitude V_{G_0} , the larger is the energy difference between the simple commensurate and the HOC structures. This fact remains true for a variety of adsorbate-adsorbate lateral interaction models. On the contrary, by including the second atom-surface Fourier term, the commensurate structure becomes the most stable one, even when its coefficient is two magnitudes smaller than V_{G_0} . In conclusion, it seems that the mechanism of stabilization of HOC structures with several atoms per unit cell is exclusively due to the contribution of corresponding high-order Fourier terms, at least for an infinite monolayer model. In real experiments, however, the finite nature of surface terraces could induce some additional effects on the monolayer alignment, as has been shown theoretically by Grey and Bohr.²²

II. METHODOLOGY

The $(\sqrt{7} \times \sqrt{7})R19.1^\circ$ cell with a three-atom basis (the (111) surface is shown in Fig. 1. The coverage of this arrangement is $\frac{3}{7}$. Assuming that the distance between particles is equal to 2, the unit cell vectors are $v_1 = (5, -\sqrt{3})$ and $v_2 = (4, 2\sqrt{3})$. The atoms are positioned at $a_1 = (3, \frac{1}{3})$, $a_2 = (5, -\sqrt{3})$, and $a_3 = (6, \frac{2}{3})$. Assuming that only first two Fourier terms from Eq. (1) contribute to the monolayer-surface interaction, the first Fourier term vanishes for this perfect hexagonal arrangement and the most stable translational possibility is determined by the sign of the second Fourier coefficient: for $V_{\sqrt{3}G_0} < 0$ the most stable structure is the one depicted in Fig. 1(a), while for $V_{\sqrt{3}G_0} > 0$ it is the one in Fig. 1(b). The structure in Fig. 1(b) can be obtained from the structure in Fig. 1(a) by a rigid translation of $\frac{2}{3}$ in reduced unit cell units in x direction.

In order to test if this simple arrangement is stable for different interaction models, we construct several hexagonal unit cells with the same degree of coverage as the $(\sqrt{7} \times \sqrt{7})R19.1^\circ$ one. These cells are characterized by different number of adsorbate N_{ads} and substrate N_{sub} particles, but always preserve the $N_{\text{ads}}/N_{\text{sub}}$ ratio equal to $\frac{3}{7}$. Throughout this paper, they will be called $C_{\frac{N_{\text{ads}}}{N_{\text{sub}}}}$. The particular cells chosen for this study were $C_{\frac{3}{7}}$, corresponding to $(\sqrt{7} \times \sqrt{7})R19.1^\circ$, $C_{\frac{9}{21}}$, $C_{\frac{12}{28}}$, $C_{\frac{21}{49}}$, $C_{\frac{27}{63}}$, and $C_{\frac{36}{84}}$.

For lateral interactions in the monolayer, simple pairwise exponential repulsion $A \exp(-Bx)$ (Ref. 23) and the HFD-B2 model for Xe-Xe interactions²⁴ have been used. The former is supposed to favor the formation of rigid hexagonal structures, while the latter is a potential for a real system, which possess repulsive and attractive regions. The effect of McLachlan substrate-mediated dispersion term²⁵ has also been tested on the energy of different structures. The values for the HFD-B2 potential and McLachlan dispersion parameters are taken from Ref. 26 for Xe-Xe and Xe-Pt(111) interactions, respectively. The values of A and B parameters were chosen to be 8×10^5 and 4, respectively.²³ A range of values of B was tested with same results. The calculation of the lateral potential was done inside a radius of up to 20 substrate lattice constants.

The HFD-B2 potential has been frequently employed for the description of real rare-gas systems in solid state and adsorbed on surfaces. However, its validity for Xe monolayer adsorbed on Cu surfaces has been recently questioned,¹⁷⁻¹⁹ because of difference in the experimental and HFD-B2 predicted force constant between adsorbed Xe atoms. However, at least for the Xe-Pt(111) system, the HFD-B2 potential augmented by McLachlan dispersion term seems to be in very good agreement with experimental results as evidenced by several theoretical studies.^{26,27} Furthermore, recent *ab initio* calculations on the Xe monolayer are in very good agreement with the HFD-B2 model.²⁸ On the other hand, the exponential term is one of the simplest models that can be employed for description of lateral interactions in the monolayer. However, recently it has been used for the study of structures of iodine adsorbed on the Pt(111) surface.²³ The usage of the exponential term should be justified when a small coverage range is studied, as the A and B parameters can be tuned to represent a correct force constant for a given distance of the atoms in the monolayer.

In order to determine the most stable structure, we have performed a large number of conjugate-gradient optimizations starting from different random configurations for each unit cell. In the case of cells with a large number of particles, a sufficient number of runs has been performed to assure that the global minimum was found in each case.²⁹ Three different sets of runs were performed. First, a one-term Fourier expansion was used and the value of V_{G_0} was changed from -1.11 to -11.1 meV.³⁰ This V_{G_0} interval corresponds to surface potential corrugation from 10 to 100 meV. Secondly, we set $V_{G_0} = -1.11$ meV and the second Fourier coefficient was changed from 0.0055 to 0.111 meV. Thirdly, we set $V_{G_0} = -1.11$ meV and the second Fourier coefficient was changed from -0.0055 meV to -0.111 meV. All runs were

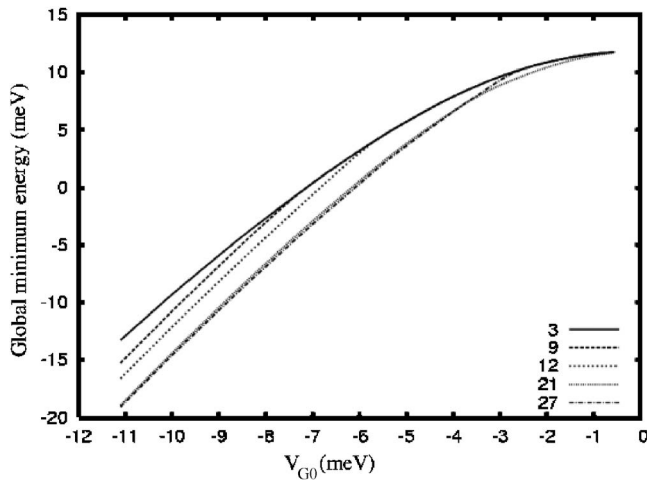


FIG. 2. Global minimum energy vs V_{G_0} for C_7^3 , C_{21}^9 , C_{28}^{12} , C_{49}^{21} , and C_{63}^{27} cells for exponential lateral interaction model.

repeated with the exponential, HFD-B2 and HFD-B2 including McLachlan dispersion term lateral interaction models. All energies in this work are reported per adsorbate particle.

III. RESULTS

In the first set of runs, for $V_{G_0} \geq -2.22$, the most stable arrangement for C_7^3 , C_{21}^9 , C_{28}^{12} , C_{63}^{27} , and C_{84}^{36} cells was the three-atom per unit cell commensurate $(\sqrt{7} \times \sqrt{7})R19.1^\circ$ structure, similar to that shown in Fig. 1(b). A perfect hexagonal structure would have all interatomic distances equal to 3.055. However, as mentioned earlier, the first Fourier term vanishes for a perfect hexagonal structure with more than one atom per unit cell, therefore the stable structure is not rigid, having interatomic distances from 2.9 to 3.2 for $V_{G_0} = -2.22$ and exponential repulsion. Interestingly, the minimum was *exactly* the same for all cells mentioned above, i.e., the stable structure in larger cells could be obtained by simply expanding the configuration of the C_7^3 cell. In this structure, all atoms are positioned relatively close to the top site and it is geometrically flat. Its stability is easily explained by the fact that the most stable site for the negative values of V_{G_0} is on-top of the substrate atom. This would seem to provide the rationale for the $(\sqrt{7} \times \sqrt{7})R19.1^\circ$ structure with all atoms close to the on-top position to be the most stable one for coverage $\frac{3}{7}$. Figure 2 shows the plot of global minimum energy vs V_{G_0} for several cells studied in this work for exponential lateral interaction model. It can be seen that the global minimum for C_{21}^9 and C_{28}^{12} cells coincides with the C_7^3 one up to $V_{G_0} = -6.11$. However, for each high-order cell, there exists a critical value of V_{G_0} after which a HOC minimum appears that is lower in energy than the simple three-atom $(\sqrt{7} \times \sqrt{7})R19.1^\circ$ one. It is interesting to note that the global minimum energy in each unit cell depends smoothly on V_{G_0} and can be characterized by a power-law behavior.

For all values of V_{G_0} employed in this study, the global minimum of the C_{49}^{21} cell always had lower energy than the

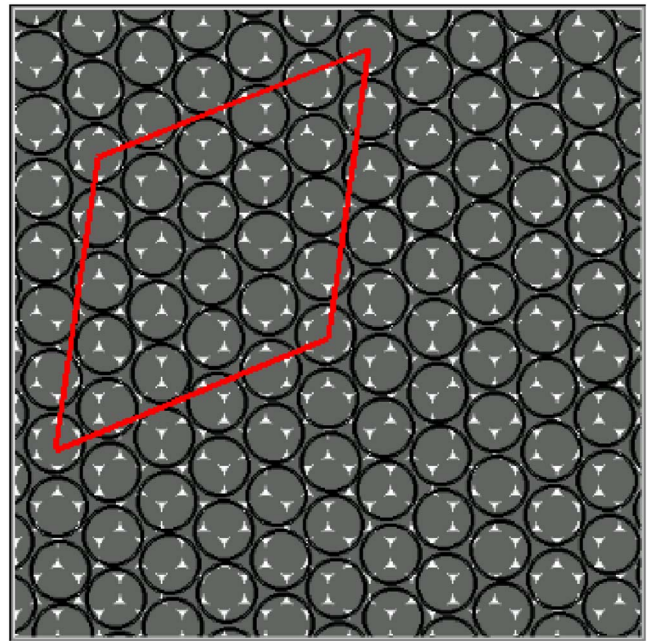


FIG. 3. (Color online) Model of a typical stable high-order commensurate structure in the C_{49}^{21} cell. The filled gray circles indicate the substrate atoms [(111) surface], while bigger black circles show adsorbate atoms. The unit cell is indicated by a red (dark gray) rhomb. Note the lower symmetry of this structure in comparison to the one depicted in Fig. 1(b).

$(\sqrt{7} \times \sqrt{7})R19.1^\circ$ one. Based on this fact, our further study will be concentrated on comparison of stable structures between these two cells exclusively. A model for typical HOC structure in the C_{49}^{21} cell is depicted on Fig. 3. In the case of HFD-B2 lateral interaction, the difference in energy between the C_7^3 minimum and the C_{49}^{21} minimum rises from 0.03 meV for $V_{G_0} = -1.11$ to 2.5 meV for $V_{G_0} = -11.1$. The energy difference curves vs V_{G_0} value for three lateral interaction models employed in this study are presented in Fig. 4. It can be seen that an increase in the value of V_{G_0} makes the global minimum in the C_{49}^{21} cell more stable than the simple commensurate $(\sqrt{7} \times \sqrt{7})R19.1^\circ$ one. This fact is surprising at first glance. Usually, one would expect the lower-order commensurate structures to be more stable due to the increased corrugation of the monolayer-surface potential.³¹ However, the contrary is found for three different lateral interaction models, from simple repulsive exponential to a real HFD-B2 model. We made additional tests with smaller B value for the $A \exp(-Bx)$ repulsion. The decrease of B makes the interaction more repulsive. Even for small values of B , the HOC structure was more stable than the simple commensurate one.

The second set of runs was performed for $V_{G_0} = -1.11$ meV and the second Fourier coefficient $V_{\sqrt{3}G_0}$ was changed from 0.006 to 0.111 meV. For HFD-B2 interaction model, the commensurate $(\sqrt{7} \times \sqrt{7})R19.1^\circ$ structure in Fig. 1(b) was stable in the C_{49}^{21} cell for $V_{\sqrt{3}G_0} > 0.01$, while for $V_{\sqrt{3}G_0} < 0.01$ the HOC structure similar to that of Fig. 3 was the most stable. With HFD-B2 lateral interaction, the stable structure had almost rigid hexagonal order with interatomic distances between 3.04 and 3.06. The results were very simi-

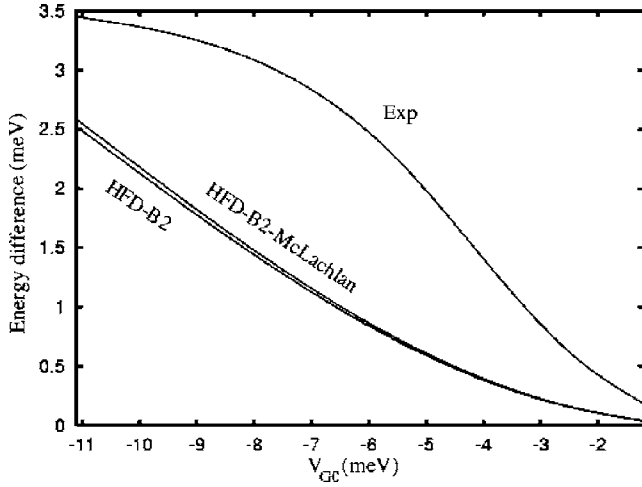


FIG. 4. Energy difference for global minima between $C_{7}^{\frac{3}{7}}$ and $C_{49}^{\frac{21}{49}}$ cells vs V_{G_0} value. The three curves are for the exponential, HFD-B2 and HFD-B2 including McLachlan substrate-mediated dispersion lateral interaction models. The curves should be interpreted from right to left, i.e., the $|V_{G_0}|$ value is increased from right to left.

lar for the HFD-B2 model with McLachlan interaction included. In the case of exponential repulsion, the simple commensurate structure was stable for $V_{\sqrt{3}G_0} > 0.05$.

In the third set of runs, we set $V_{G_0} = -1.11$ meV and the second Fourier coefficient $V_{\sqrt{3}G_0}$ was changed from -0.0055 to -0.111 meV. For HFD-B2 interaction model, the commensurate $(\sqrt{7} \times \sqrt{7})R19.1^\circ$ structure in Fig. 1(a) was stable in the $C_{49}^{\frac{21}{49}}$ cell for $V_{\sqrt{3}G_0} < -0.02$, while for $V_{\sqrt{3}G_0} > -0.02$ the HOC structure in Fig. 4 was the most stable. The results were almost equal for the HFD-B2 model with McLachlan interaction included. In the case of exponential repulsion, the simple commensurate structure was stable for $V_{\sqrt{3}G_0} < -0.07$. It is interesting to note that for HFD-B2 interaction even when $V_{\sqrt{3}G_0}$ is two magnitudes smaller than V_{G_0} , the stable structure changes from the one shown on Fig. 1(b) to that shown in Fig. 1(a) for all cells studied, due to the effect of negative $V_{\sqrt{3}G_0}$.

In order to test how general are the conclusions of the present study, an additional simulation of stable structures for a commensurate (3×3) cell with four atoms basis has been performed. The results indicate similar behavior as for the $(\sqrt{7} \times \sqrt{7})R19.1^\circ$ case. A larger $C_{63}^{\frac{28}{63}}$ cell could be found with same coverage as (3×3) , which contains a minimum with lower energy and lower symmetry than the (3×3) one. However, including the Fourier term with third shell of reciprocal cell vectors makes the commensurate (3×3) structure the most stable one. Additionally, simulations have been carried out in a large $C_{343}^{\frac{147}{343}}$ cell with $\theta = \frac{3}{7}$. It was found that, for one Fourier component model, the most stable structure had lower energy than the one in $C_{49}^{\frac{21}{49}}$ cell. However, including the second Fourier term made the $(\sqrt{7} \times \sqrt{7})R19.1^\circ$ structure with three-atom basis stable in the large $C_{343}^{\frac{147}{343}}$ cell.

IV. DISCUSSION

In what follows I will attempt to provide a physical justification for the stabilization of the high-order commensurate

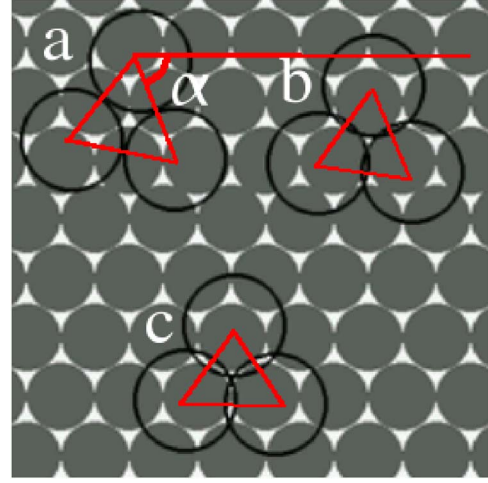


FIG. 5. (Color online) Illustration of the triangle formed by three atoms due to the high degree of symmetry in the $(\sqrt{7} \times \sqrt{7})R19.1^\circ$ unit cell for (a) $V_{G_0} = -0.111$, (b) $V_{G_0} = -5.55$, (c) $V_{G_0} = -11.1$ meV and exponential repulsion. The simulations were performed using a periodic model. The (equilateral) triangle side length and angle α formed between a horizontal line and one side of the triangle are 3.06 and 70.9° , 2.76 and 65.8° , 2.63 and 62.6° , for (a), (b), and (c), respectively.

structure instead of the three-atom commensurate one with increase in V_{G_0} and the reversed stability of the simple commensurate structure when the second Fourier term contribution is included. In our model (assuming exponential lateral interaction), the global minimum energy in each unit cell is a function of three parameters V_{G_0}/A , $V_{\sqrt{3}G_0}/A$, and B . Let us assume that only V_{G_0} is changed, with $V_{\sqrt{3}G_0} = 0$ and $B > 0$ is kept constant. For negligible V_{G_0} , the global minimum in any cell with $\theta = \frac{3}{7}$ would be a trivial structure with perfect hexagonal symmetry and interatomic distance $d = 3.055$. The dependence of the global minimum energy on V_{G_0} is depicted in Fig. 2. If the geometry of the global minimum were kept fixed, one would expect a linear $E(V_{G_0})$ behavior. Therefore, the power-law $E(V_{G_0})$ dependence in Fig. 2 is due to considerable geometry relaxation with an increase in corrugation, which is also apparent from the simulation results and such a process is illustrated in Fig. 5. For small (compared with the repulsive force) $V_{G_0} < 0$, the most stable structure in the $C_{7}^{\frac{3}{7}}$ cell is the one shown in Fig. 1(b) [periodic model] and Fig. 5(a) [a triangle within one unit cell]. For large $V_{G_0} < 0$, the most stable structure can be obtained from that in Fig. 5(a) by rotating and compressing the triangle formed by three adsorbate atoms inside the unit cell until all of them are positioned directly on top of a triangle formed by three substrate atoms [similar to Fig. 5(c)]. This configuration optimizes the monolayer-surface interaction at expense of the repulsive lateral interaction.

Decreasing B in $A \exp(-Bx)$ has an opposite effect: it drives the monolayer to adopt a perfect hexagonal arrangement, thus decreasing the monolayer-surface interaction. From this discussion, a simple physical picture emerges for the stabilization of HOC structures with an increase in V_{G_0} : it is due to the strain relief mechanism (or equivalently, sym-

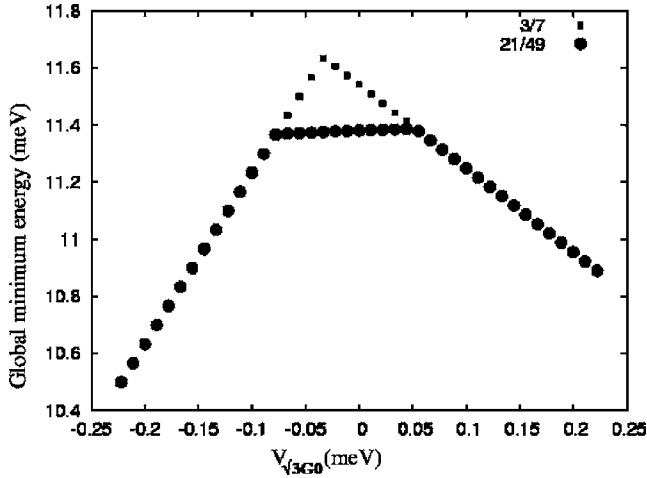


FIG. 6. Global energy minimum vs $V_{\sqrt{3}G_0}$ for $C_{7/7}$ and $C_{21/49}$ cells ($V_{G_0} = -1.11$).

metry breaking) which optimizes the lateral interactions in the monolayer. This is also clearly seen from Fig. 2: if $N_{\text{ads},1} > N_{\text{ads},2}$, there exists a value of V_{G_0} from which the global minimum of a cell with $N_{\text{ads},1}$ is more stable than the one of the cell with $N_{\text{ads},2}$. Evidently, the higher symmetry of cells with low N_{ads} implies higher global minimum energy.

The other issue which still lacks explanation is why the second Fourier term favors the commensurability once again. As shown in Ref. 20, the second Fourier term is fully conserved for a perfect hexagonal arrangement with three atoms per unit cell [e.g., the $(\sqrt{7} \times \sqrt{7})R19.1^\circ$ structure]. Therefore, it is expected that its inclusion will drive the monolayer to recover the hexagonal structure with higher symmetry. In order to investigate the mechanism of this process, we have performed simulations in $C_{7/7}$ and $C_{21/49}$ cells for $V_{G_0} = -1.11$ and $-0.222 \leq V_{\sqrt{3}G_0} \leq 0.222$. The global minimum energy vs $V_{\sqrt{3}G_0}$ plot for these two cells is shown on Fig. 6. The first thing to note is the linear behavior of the global minimum energy vs $V_{\sqrt{3}G_0}$. In the case of $C_{7/7}$ cell, two different lines can be observed: the one on the left side for structure in Fig. 1(a) and the one on the right side for structure in Fig. 1(b). The linear behavior indicates that the geometry is affected negligibly upon the inclusion of the second Fourier term (at least up to $|V_{\sqrt{3}G_0}| = 0.2|V_{G_0}|$), which is also observed after analyzing the global minimum coordinates for different values of $V_{\sqrt{3}G_0}$. The variation in the slope of the curves can be explained by characteristically different geometries of the global minima. In the case of $C_{7/7}$ cell, the structure in the right part of the curve contains only one geometrically distinct site [asymmetric in Fig. 1(b)], while the structure on the left possesses two different sites: one on-top and two three-fold hollow sites [Fig. 1(a)]. Thus, the contribution to the total energy with variation in $V_{\sqrt{3}G_0}$ is not equal for both structures, giving origin to differences in the slope.

Additionally, a new global minimum appears in the $C_{21/49}$ cell when compared to the $C_{7/7}$ cell: it is the HOC structure (Fig. 3), which is more stable than the simple $(\sqrt{7} \times \sqrt{7})R19.1^\circ$ for a small interval of $V_{\sqrt{3}G_0}$ as already shown previously in this work. The relatively complex geometry of

the HOC structure in the $C_{21/49}$ cell (Fig. 3) leads to slightly positive slope from $V_{\sqrt{3}G_0} = -0.066$ to $V_{\sqrt{3}G_0} = 0.044$ and loses its stability to the highly symmetric $(\sqrt{7} \times \sqrt{7})R19.1^\circ$ arrangement outside of that region with a second order phase transition.

It is important to mention that the evidence of the influence of the second Fourier term given above is for small corrugation of the atom-surface potential ($V_{G_0} = -1.11$), for which the atomic relaxation inside the $C_{7/7}$ cell is small (the distance between the atoms in the triangle is 2.98). For large values of V_{G_0} , the relaxation becomes more important and the ratio $V_{\sqrt{3}G_0}/V_{G_0}$ needed to stabilize the simple $(\sqrt{7} \times \sqrt{7})R19.1^\circ$ structure grows. We performed selective simulations for $V_{G_0} = -11.1$ and variable $V_{\sqrt{3}G_0}$ and found that in that case, the increase of $V_{\sqrt{3}G_0}$ has a pronounced non-linear effect on the geometry inside the $C_{7/7}$ cell, driving the monolayer to recover the hexagonal arrangement. Thus, one can conclude that for certain $V_{\sqrt{3}G_0}/V_{G_0}$ threshold, the behavior of the global minimum energy versus $V_{\sqrt{3}G_0}$ becomes nonlinear, in contrast to what is shown in Fig. 6 for $V_{G_0} = -1.11$.

Analyzing the results above, I believe that enough evidence has been collected to show that specific high-order Fourier terms are mandatory for appearance of commensurate structures. Even if the magnitude of those terms is very small, they determine the stability of the commensurate structures. However, the precise stability of commensurate structures in respect to incommensurate ones is due to the interplay of the monolayer-surface and the lateral monolayer interactions. This fact could be illustrated by comparing the results for exponential and HFD-B2 lateral interaction models. In the case of exponential repulsion (with A and B values chosen in this work), it would require higher $V_{\sqrt{3}G_0}/V_{G_0}$ ratio to make the $(\sqrt{7} \times \sqrt{7})R19.1^\circ$ structure the most stable one. On the basis of rationalization provided above, this can be explained as follows: higher repulsion of the HFD-B2 interaction as compared to the exponential model undermines the effect of the first Fourier term by favoring the hexagonal monolayer arrangement, thus requiring smaller $V_{\sqrt{3}G_0}/V_{G_0}$ ratio for the stabilization of the simple commensurate structure. However, a sufficiently small value of B in the exponential model would have exactly the same consequences.

V. CONCLUDING REMARKS

Detailed analysis of the role of higher-order atom-surface potential Fourier terms has been performed for several unit cells with $\theta = \frac{3}{7}$ and evidence has been presented indicating their importance for the stability of commensurate structures. The commensurate structures become stable even when the value of the corresponding higher-order Fourier coefficient is very small. The largest unit cell analyzed in detail in this work consists of 36 adsorbate atoms. While it is possible that lower energy higher-order commensurate structures could exist in larger cells, an increase of corresponding Fourier coefficient is still expected to stabilize the simple commensurate structure. It would be appealing to make a systematic

study up to a certain high-order Fourier term. Furthermore, the global minimum energy in all cells studied in this work seems to be well-behaved in respect to the interaction potential parameters, which indicates on the possibility of an analytical treatment.

ACKNOWLEDGMENTS

Fruitful discussions with Marcelo Galván and Nikola Batina are acknowledged. Financial support was provided by CONACYT. Calculations were performed at LSVP in UAM-Iztapalapa.

*Electronic address: sanix@ixil.izt.uam.mx

- ¹G. A. Somorjai, *Introduction to Surface Chemistry and Catalysis* (Wiley, New York, 1994).
- ²D. E. Hooks, T. Fritz, and M. D. Ward, *Adv. Mater. (Weinheim, Ger.)* **13**, 227 (2001).
- ³A. D. Novaco and J. P. McTague, *Phys. Rev. Lett.* **38**, 1286 (1977).
- ⁴J. P. McTague and A. D. Novaco, *Phys. Rev. B* **19**, 5299 (1979).
- ⁵R. D. Diehl, T. Seyller, M. Caragiu, G. S. Leatherman, N. Ferralis, K. Pussi, P. Kaukasoina, and M. Lindroos, *J. Phys.: Condens. Matter* **16**, 2839 (2004).
- ⁶O. M. Magnussen, *Chem. Rev. (Washington, D.C.)* **102**, 679 (2002).
- ⁷R. D. Diehl and R. McGrath, *J. Phys.: Condens. Matter* **9**, 951 (1997).
- ⁸A. Patrykiewicz, S. Sokolowski, and K. Binder, *Surf. Sci. Rep.* **37**, 207 (2000).
- ⁹A. Patrykiewicz, S. Sokolowski, and K. Binder, *J. Chem. Phys.* **115**, 983 (2001).
- ¹⁰R. Bennewitz, J. N. Crain, A. Kirakosian, J.-L. Lin, J. L. McChesney, D. Y. Petrovykh, and F. J. Himpsel, *Nanotechnology* **13**, 499 (2002).
- ¹¹L. W. Bruch, M. W. Cole, and E. Zaremba, *Physical Adsorption: Forces and Phenomena* (Oxford University Press, New York, 1997).
- ¹²W. A. Steele, *Surf. Sci.* **36**, 317 (1973).
- ¹³J. E. Black and A. Janzen, *Phys. Rev. B* **38**, 8494 (1988).
- ¹⁴J. E. Black and A. Janzen, *Phys. Rev. B* **39**, 6238 (1989).
- ¹⁵In the case of rare-gas monolayer on (111) metal surfaces, the $(\sqrt{3} \times \sqrt{3})R30^\circ$ structure would be the ground state provided that V_{G_0} is sufficiently large.
- ¹⁶P. Zeppenfeld, U. Becher, K. Kern, and G. Comsa, *Phys. Rev. B* **45**, 5179 (1992).
- ¹⁷J. Braun, D. Fuhrmann, A. Siber, B. Gumhalter, and C. Wöll, *Phys. Rev. Lett.* **80**, 125 (1998).
- ¹⁸C. Boas, M. Kunat, U. Burghaus, B. Gumhalter, and C. Wöll, *Phys. Rev. B* **68**, 075403 (2003).
- ¹⁹A. Siber, B. Gumhalter, J. Braun, A. P. Graham, M. Bertino, J. P. Toennies, D. Fuhrmann, and C. Wöll, *Phys. Rev. B* **59**, 5898 (1999).
- ²⁰A. Tkatchenko, *Phys. Rev. B* **74**, 035428 (2006).
- ²¹L. W. Bruch, *Phys. Rev. B* **37**, 6658 (1988).
- ²²F. Grey and J. Bohr, *Europhys. Lett.* **18**, 717 (1992).
- ²³A. Tkatchenko, N. Batina, and M. Galvan, *Phys. Rev. Lett.* **97**, 036102 (2006).
- ²⁴A. K. Dham, W. J. Meath, A. R. Allnatt, R. A. Aziz, and M. J. Slaman, *Chem. Phys.* **142**, 173 (1990).
- ²⁵A. D. McLachlan, *Mol. Phys.* **7**, 381 (1964).
- ²⁶L. W. Bruch, A. P. Graham, and J. P. Toennies, *J. Chem. Phys.* **112**, 3314 (1999).
- ²⁷R. D. Boutchko and L. W. Bruch, *Phys. Rev. B* **70**, 195422 (2004).
- ²⁸P. Lazić, Ž. Črljen, R. Brako, and B. Gumhalter, *Phys. Rev. B* **72**, 245407 (2005).
- ²⁹It was found that the number of distinct local minima in our study was not large even for the cell with 36 adsorbate particles. The exploration of the potential energy surface was considered complete when no new minima could be identified in 500 conjugate-gradients minimizations. The total number of minimizations for the C_{84}^{36} cell was around 2000.
- ³⁰The minus sign was used for the first Fourier coefficient to make the atop site the most stable on the (111) surface. The chosen interval corresponds to the atop site energy from 10 to 100 meV respective to the least stable fcc adsorption site.
- ³¹L. W. Bruch, *Phys. Rev. B* **64**, 033407 (2001).